5th Meeting of the Scientific Committee

Shanghai, China
23 - 28 September 2017

SC5-SQ02

A Stock assessment of the jumbo flying squid (*Dosidicus gigas*) in Southeast Pacific Ocean (2017)

Luoliang Xu, Bai Li, Gang Li, Xinjun Chen & Yong Chen

A Stock assessment of the jumbo flying squid (*Dosidicus gigas*) in Southeast Pacific Ocean (2017)

Luoliang Xu[1,2], Bai Li[2], Gang Li[1], Xinjun Chen[1], Yong Chen[2,1]

[1]College of Marine Sciences, Shanghai Ocean University, Shanghai, China
[2]School of Marine Sciences, University of Maine, Orono, Maine 04469, USA

Introduction

Jumbo flying squid, *Dosidicus gigas* (d'Orbigny 1835), is widely distributed in the eastern Pacific Ocean (Nigmatullin et al., 2001). Jumbo flying squid in the Southeast Pacific supports the largest squid fishery in the world. The catch surpassed one million metric ton in 2014 (FAO, Figure1). There are seven fishing entities targeting *Dosidicus gigas* in Southeast Pacific Ocean. The whole fishing ground of jumbo flying squid in this area was approximately located in the area of 0°~30°S, 70°~90°W. Peru and Chile are fishing in their own Exclusive Economic Zone (EEZ) while the other four fishing entities are fishing on high seas. Three sub-unit stocks of jumbo flying squid in Southeast Pacific has been identified by the distinguishable sizes at which individuals reach maturity (Nigmatullin et al., 2001). However no relevant genetic differences have been found between the three sub-unit populations proposed by Nigmatullin (Sandoval-Castellanos et al., 2010). There has been limited effort for a formal assessment of this stock so far. In this report, the standardized catch per unit effort (CPUE) data of Chinese vessels were used as biomass abundance indices in a state-space surplus production model developed to describe the dynamics of this stock.

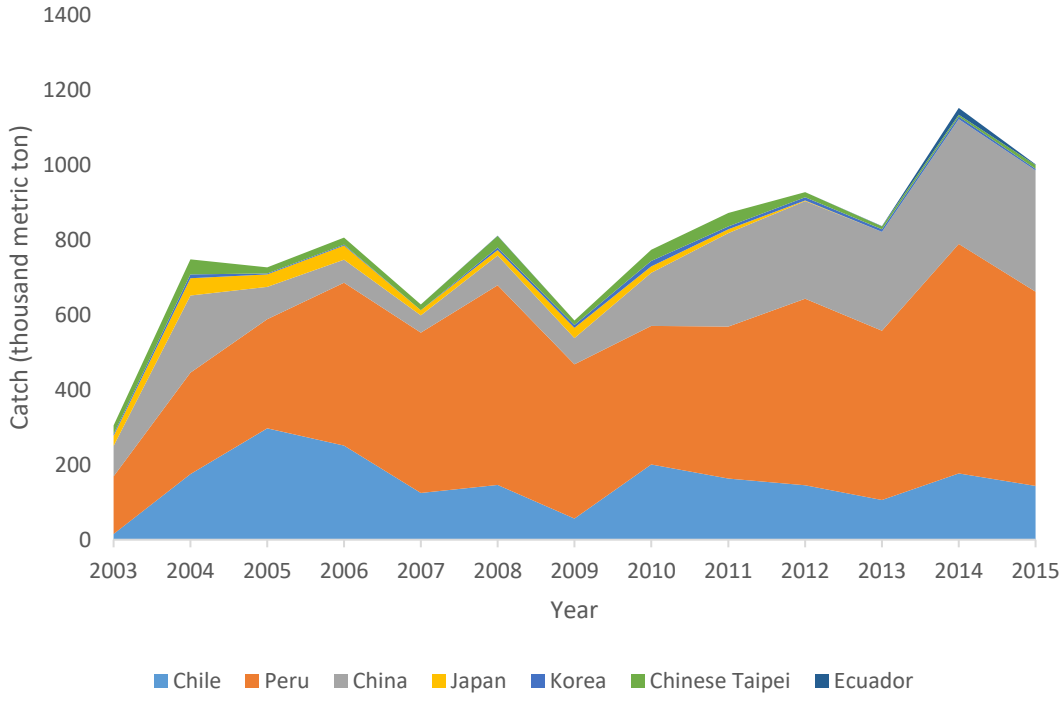

Figure 1. Catch of jumbo flying squid in Southeast Pacific Ocean by 6 fishing entities from 2000 to 2015

Population structure

Nigmatullin et al (2001) identified three intraspecific groups distinguished by different sizes at which individuals reach maturity. The group that mature at small size (130-260 mm ML for male and 140-340 mm ML for female) was found predominantly in the area near equator. The group that mature at medium size (240-420 mm ML for male and 280-600 for female) was found over the whole species range except at the higher latitude. The group that mature at large size (over 400 for male and over 550 for female) occurred at the northern and southern peripheries of the species range and the international water off Peruvian EEZ (Liu et al., 2013; Nigmatullin et al., 2001). The three groups fully or partially overlapped throughout the fishing grounds. Although no genetic differences were found amongst the three size groups (Sandoval-Castellanos et al., 2010), we could not exclude the possibility of the Southeast Pacific jumbo flying squid population being formed by multiple self-sustained stock units with distinct and independent reproductive and growth processes (Csirke et al., 2015). It was found that the lower temperature water which jumbo flying squid come across in early life stage may stimulate the individual to significantly grow larger, live longer and mature later (Arkhipkin et al., 2014). Thus the environmental variability might partially explain why the population structure of jumbo flying squid was so complex and unstable.

We believe that an assumption of multiple populations could better reflect the reality of dynamic of jumbo flying squid in Southeast Pacific. However, the catch and abundance index data currently available to this study only include total catch and CPUE which are not classified by the size groups. We may as well assume that the jumbo flying squid in Southeast Pacific is a single stock in this study for the purpose of stock assessment.

Data used in the stock assessment

Fishery-dependent data

(1) Catch data

Catch data of jumbo flying squid in the Southeast Pacific Ocean during 2003~2015 were derived from Food and Agriculture Organization (FAO) of United Nation (UN) database (www.fao.org/fishery/statistics/global-capture-production/query/en; accessed on

06/26/2017). The catch by different fishing entities occurred throughout the whole fishing ground in Southeast Pacific including EEZ of Peru and Chile as well as the adjacent international water (Table 1).

Table 1. Jumbo flying squid catches (thousand metric ton) in the Southeast Pacific Ocean by fishing entities from 2003 to 2015

Year	Chile	Peru	China	Japan	Korea	Chinese Taipei	Ecuador	Total
2003	15.191	153.727	81	27.058	4.722	23.009	0	304.707
2004	175.134	270.368	205.6	46.187	10.787	39.45	0	747.526
2005	296.954	291.14	86	33.652	2.519	15.976	0	726.241
2006	250.989	434.261	62	37.428	2.485	18.349	0.212	805.724
2007	124.389	427.591	46.4	14.059	0	14.75	0.121	627.31
2008	145.667	533.414	79.064	14.143	6.775	31.161	0.668	810.892
2009	56.337	411.805	70	27.271	7.221	12.319	0	584.953
2010	200.428	369.822	142	17.113	14.506	29.206	0	773.075
2011	163.495	404.73	250	9.977	7.843	35.418	0	871.463
2012	144.965	497.462	261	1.448	8.31	14.177	0.091	927.453
2013	106.271	451.061	264	0	7.067	7.759	0.002	836.16
2014	176.602	612.444	332.523	0	7.203	4.795	18.146	1151.713
2015	143.684	517.974	323.636	0	4.263	10.072	1.279	1000.908

(2) Abundance index data

The abundance index data (CPUE) were from Squid jigging technical group of China Distant Water Fisheries Association. The data field consisted of fishing time (month), fishing area (0.25° longitude ×0.25° latitude) and yield. The nominal CPUE is calculated as follows:

$$Nominal\ CPUE_{y,m,i,j} = Catch_{y,m,i,j} / Effort_{y,m,i,j} \quad (1)$$

where $Catch_{y,m,i,j}$ was the total catch occurred in year y, month m, latitude i and longitude j. $Effort_{y,m,i,j}$ and $Nominal\ CPUE_{y,m,i,j}$ were the total fishing efforts and nominal CPUE, respectively, in the specified spatial grid at the specified time.

The nominal CPUE was standardized by Generalized Linear Model (GLM). The expression of GLM is as follows:

$$ln(Nominal\ CPUE + \sigma) = k + \sum\ （a_i \times x_i）+ \varepsilon \quad (2)$$

the value of σ is 10% of nominal CPUE mean which was added to deal with the 0 value of nominal CPUE. k is the intercept. x_i is an independent variable including environmental factors (i.e. sea surface temperature, concentration of chlorophyll-a) and spatial-temporal factors (i.e. year, month, longitude, latitude). a_i is the related coefficient. ε is the error term which is assumed to follow normal distribution. Environmental data came from remote sensing satellite dataset in National Oceanic and Atmospheric Administration (NOAA) database (http://pifsc-oceanwatch.irc.noaa.gov/erddap/index.html, accessed on 06/28/2017). Sea surface temperature (SST) and concentration of chlorophyll-a (Chl-a) were chosen because these environmental factors were found to greatly affect the jumbo flying squid's habitat and will subsequently influence the fish aggregation and the fishing efficiency (Yu et al., 2016).

The results of GLM is shown in Table 2. The trends of standardized CPUE and the nominal CPUE are consistent (Figure 2). The standardized CPUE was used as an abundance index in the surplus production stock assessment model.

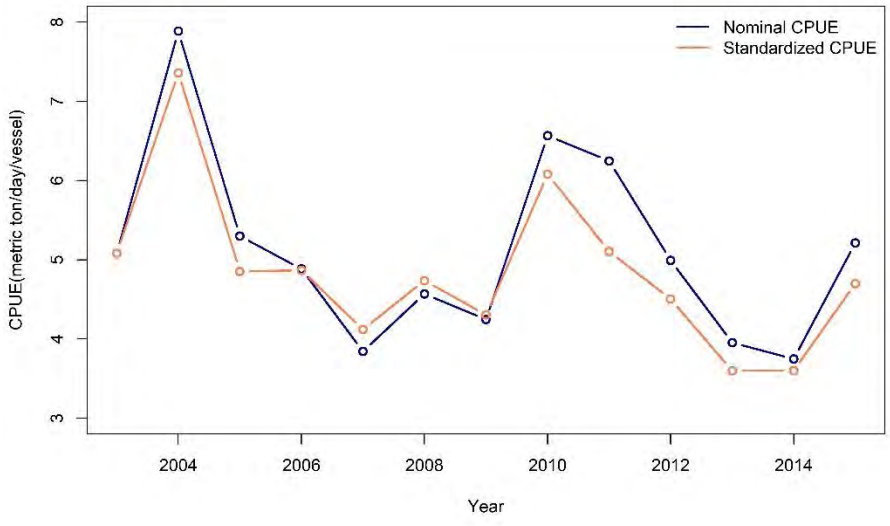

Figure 2. Nominal CPUE and standardized CPUE of jumbo flying squid fished by Chinese jigging vessels from 2003 to 2015

Table 2. The summaries of results of GLM used to standardize nominal CPUE

Factors	Estimate	Std. Error	t value	Pr(>|t|)
Intercept	1.9000	0.1524	12.4643	0.0000
Year 2004	0.3699	0.0421	8.7976	0.0000
2005	-0.0466	0.0540	-0.8624	0.3885
2006	-0.0436	0.0547	-0.7964	0.4258
2007	-0.2102	0.0532	-3.9546	0.0001
2008	-0.0707	0.0405	-1.7466	0.0807
2009	-0.1665	0.0423	-3.9329	0.0001
2010	0.1789	0.0466	3.8406	0.0001
2011	0.0040	0.0366	0.1088	0.9134
2012	-0.1209	0.0378	-3.1954	0.0014
2013	-0.3451	0.0357	-9.6777	0.0000
2014	-0.3451	0.0364	-9.4859	0.0000
2015	-0.0788	0.0364	-2.1648	0.0304
Month 2	-0.2953	0.0242	-12.1866	0.0000
3	-0.5581	0.0235	-23.7976	0.0000
4	-0.6365	0.0246	-25.8862	0.0000
5	-0.5242	0.0241	-21.7100	0.0000
6	-0.5190	0.0235	-22.1130	0.0000
7	-0.3956	0.0223	-17.7581	0.0000
8	-0.2744	0.0229	-11.9840	0.0000
9	-0.2672	0.0237	-11.2618	0.0000
10	-0.0736	0.0241	-3.0550	0.0023
11	0.0096	0.0249	0.3846	0.7005
12	0.0353	0.0253	1.3958	0.1628
lon	-0.0013	0.0017	-0.7791	0.4360
lat	-0.0037	0.0013	-2.7367	0.0062
sst	0.0000	0.0000	-1.7454	0.0809
chla	0.0000	0.0000	2.1647	0.0304

Fishery-independent data

Inaccessible now.

Stock assessment model

Description of Bayesian state-space surplus production model

A complete operational surplus production model consists of two parts, i.e. dynamic model which describe the recruitment, growth and mortality of the stock and observation model which relates observation (e.g. CPUE or abundance index by scientific survey) to the stock biomass.

The form of dynamic model is as follows:

$$B_{y+1} = \left(B_y + g\left(B_y\right) - C_y\right)e^{\varepsilon_y} \quad (3)$$

where B_y is the biomass at the beginning of year y; C_y is catch in year y; I_y is the index of abundance for year y; ε_y is process error which follows normal distribution (e.g. $\varepsilon_y \sim N(0,\sigma_\varepsilon^2)$); $g(B_y)$ is surplus production as a function of B_y and the Schaefer's form is

$$g\left(B_y\right) = rB_y\left(1 - \frac{B_y}{k}\right) \quad (4)$$

where r is the intrinsic growth rate and k is the capacity denoting the unexploited biomass size.

Pella and Tomlinson considered an extension of Schaefer model:

$$g\left(B_y\right) = rB_y\left(1 - \frac{B_y}{k}\right)^s \quad (5)$$

equation (4) and (5) are identical when s=1. The reason for the addition of parameter s is that in Schaefer model the surplus production is symmetric in relation to biomass whereas the Pella and Tomlinson's equation allows the relationship to be skewed (Hilborn and Walters, 1992).

The form of observation model is as follows:

$$I_y = qB_y e^{\eta_y} \quad (6)$$

where q is catchability coefficient; η_y is the observation error which follows normal distribution (e.g. $\eta_y \sim \text{normal}(0, \sigma_\eta^2)$).

State-space model predicts the future state of a system from its previous states probabilistically (Patterson et al., 2008). Process error and observation error could be

simultaneously incorporated into a state-space model. Bayesian approach has been developed to rigorously incorporate expert judgment and inferences into conventional stock assessment and has also been used to convey uncertainties in management strategies to decision maker (McAllister and Kirkwood, 1998). In this study, a Bayesian state-space Pella and Tomlinson's surplus production model was chosen to describe the fishery dynamic of jumbo flying squid in Southeast Pacific.

Prior distribution

Setting appropriate prior distribution is primary in Bayesian paradigm. One base scenario and five sensitivity analysis scenarios were set based on varied prior distribution. In base scenario, the parameters r, K and q followed uniform distribution typically used when we only have very limit information. The range of each parameter is large enough to cover the possible values. Shape parameter s followed gamma distribution and the mean of s was set to be 1. The variance of process error and observation error followed inverse gamma distribution. In sensitivity analysis scenario 1, all the other parameter's distributions were identical with those in base scenario except r following log-normal distribution. The 10% and 90% quantile of r's prior distribution were 0.12 and 3.19, respectively. And the mean of r was 1.40 in this scenario. In sensitivity analysis scenario 2, all the other parameter's distributions were identical with those in base scenario except K following log-normal distribution. The 10% and 90% quantile of K were set to be 128 and 2795 and the mean was 1231 (ten-thousand metric ton) in this scenario. In sensitivity scenario 3, both r and K were set to follow the same log-normal distributions as sensitivity scenario 1 and 2. The only difference between sensitivity scenario 1 and 4 is that in sensitivity scenario 4 parameter r was set to follow a lognormal distribution with higher mean value (1.51). In scenario 5, r and K were set to follow the same lognormal distribution with those in scenario 2 and 4 (Table 3).

Table 3. The prior distributions of parameters in base scenario and sensitivity analysis scenarios

Parameter	Base Scenario	Sensitivity analysis scenario				
		1	2	3	4	5
r	uniform (0.1,3.5)	lognormal (-0.5,1.67)	uniform (0.0001,0.1)	lognormal (-0.5,1.67)	lognormal(-0.3,1.20)	lognormal(-0.3,1.20)
K	uniform (120,3000)	uniform (0.0001,0.1)	lognormal (6.4,1.43)	lognormal (6.4,1.43)	uniform (0.0001,0.1)	lognormal (6.4,1.43)
q	uniform (0.0001,0.1)	uniform (0.0001,0.1)	uniform (0.0001,0.1)	uniform (0.0001,0.1)	uniform (0.0001,0.1)	uniform (0.0001,0.1)
s	gamma (2,2)	gamma (2,2)	gamma (2,2)	gamma (2,2)	gamma (2,2)	gamma (2,2)
tau	inverse gamma (2,0.45)	inverse gamma (2,0.45)	inverse gamma (2,0.45)	inverse gamma (2,0.45)	inverse gamma (2,0.45)	inverse gamma (2,0.45)
sigma	inverse gamma (2,0.45)	inverse gamma (2,0.45)	inverse gamma (2,0.45)	inverse gamma (2,0.45)	inverse gamma (2,0.45)	inverse gamma (2,0.45)

**tau* and *sigma* are the variances of observation error and process error, respective

Convergence test

Convergence of the MCMC samples to the posterior distribution was checked by monitoring the trace of three chains of each parameter (Figure 3). The iterations was done for 100000 times for each MCMC chain and the first half was removed. Heidelberger and Welch (1983) as well as Gelman and Rubin (1992) diagnostics were also examined. According to the results of the test, all the model runs in each scenario were converged.

Posterior distribution

For the base scenario, the mean of posterior distribution of parameters *r, K, q, s, tau, sigma* were 1.559, 1103.276 (10^4 metric ton), 0.011, 0.716, 0.121 and 0.142, respectively. The coefficient of variance of all parameters in the base scenario was less than 1 (Table 4). The significant difference between prior distribution and posterior distribution indicated that the data in the model provided sufficient information to dominate the form of posterior distribution in base scenario (Figure 4(a)). *K* and *q*, *r* and *s*, *K* and *r* showed negative relationship whereas *q* and *r* showed positive relationship (Figure 5).

Table 4. The posterior distribution statistic of parameters in base scenario and sensitivity analysis scenarios

Scenario	Statistic	*r*	*K* (10^4 metric ton)	*q*	*s*	*tau*	*sigma*
Base	mean	1.559	1103.276	0.011	0.716	0.121	0.142
	median	1.412	903.500	0.007	0.598	0.106	0.125
	mode	1.476	1307.750	0.011	1.064	0.111	0.136
	cv	0.587	0.675	0.896	0.691	0.556	0.508
Sensitivity 1	mean	0.890	1303.040	0.008	0.926	0.119	0.144
	median	0.639	1162.000	0.006	0.796	0.106	0.124
	mode	0.799	1182.667	0.006	1.025	0.105	0.127
	cv	1.068	0.584	0.852	0.665	0.492	0.535
Sensitivity 2	mean	1.789	691.461	0.017	0.774	0.118	0.140
	median	1.737	470.800	0.014	0.659	0.105	0.122
	mode	1.932	691.600	0.015	0.831	0.119	0.149
	cv	0.500	1.110	0.724	0.619	0.478	0.536
Sensitivity 3	mean	1.132	865.757	0.014	0.955	0.119	0.147
	median	0.837	629.550	0.011	0.827	0.107	0.128
	mode	1.153	1334.667	0.012	1.111	0.111	0.135
	cv	0.944	1.007	0.784	0.627	0.551	0.536
Sensitivity 4	mean	1.034	1226.171	0.009	0.916	0.115	0.141
	median	0.743	1018.500	0.006	0.778	0.103	0.121
	mode	1.058	1311.500	0.007	1.221	0.106	0.162

	cv	1.333	0.617	0.875	0.685	0.497	0.550
	mean	1.305	829.622	0.014	0.928	0.115	0.145
Sensitivity 5	median	0.978	593.850	0.011	0.814	0.104	0.125
	mode	1.369	1026.000	0.013	1.029	0.117	0.153
	cv	0.964	0.944	0.748	0.650	0.455	0.537

Biological reference points

The biological reference points are essential for figuring out the stock status and giving management advises. The three biological references (i.e. *Bmsy*, *MSY*, *Fmsy*) were calculated as follows:

$$Bmsy=K*(s+1)^{(-1/s)} \quad (7)$$

$$MSY=r*(1-1/(s+1))*Bmsy \quad (8)$$

$$Fmsy=MSY/Bmsy \quad (9)$$

For the base scenario, the biological reference points *Bmsy*, *MSY*, *Fmsy* were 519.011 (10^4 metric ton), 337.619 (10^4 metric ton) and 0.651, respectively (Table 5). Please note that *Fmsy* is not an instantaneous fishing mortality here. It is more an annual exploitation rate.

Table 5. The statistic of biological reference points in base scenario and sensitivity analysis scenarios

Scenario	Biological reference points	mean	median	mode
Base	*Bmsy*	519.011	412.544	661.857
	Fmsy	0.651	0.528	0.761
	MSY	337.619	217.852	503.652
Sensitivity 1	*Bmsy*	641.992	556.872	594.171
	Fmsy	0.428	0.283	0.404
	MSY	274.531	157.633	240.229
Sensitivity 2	*Bmsy*	329.678	218.383	334.002
	Fmsy	0.780	0.690	0.877
	MSY	257.279	150.624	292.875
Sensitivity 3	*Bmsy*	429.114	303.779	681.246
	Fmsy	0.553	0.379	0.607
	MSY	237.342	115.150	413.389
Sensitivity 4	*Bmsy*	602.904	486.129	682.206
	Fmsy	0.494	0.325	0.582
	MSY	298.029	158.157	396.742
Sensitivity 5	*Bmsy*	408.940	285.726	515.852
	Fmsy	0.628	0.439	0.694

MSY	256.869	125.434	358.148

*the unit of *Bmsy* and *MSY* is 10^4 metric ton

Stock status

The temporal trends of *Bratio* (*B/Bmsy*) and *Fratio* (*F/Fmsy*) in different scenarios showed similar patterns. The fishing mortality was increasing over the exploited history. There is no clue showing that the fishery is subject to overfishing or the stock is overfished. According the Kobe plot, the stock being overfishing or overfished had never happened since 2003 (Figure 6).

Model fitting and retrospective pattern

The predicted CPUE from model and the observed CPUE showed similar temporal trend (Figure 7). Retrospective analysis was conducted to examine the consistency of biomass and fishing mortality when successive data were incorporated into stock assessment model. The severity and direction of retrospective pattern could be quantified by Mohn's rho (Mohn, 1999).

$$\rho = \frac{\sum_{n=1}^{x}(X_{t-n,t-n} - X_{t-n,t})}{X_{t-n,t}} / x \qquad (10)$$

where $X_{t\text{-}n,t}$ is the estimate of some quantity for year t-n from a stock assessment with a terminal year of t. x is the number of years peeled off the full time series. The Mohn's rho of biomass and fishing mortality in base scenario were -0.12 and 0.14, respectively. There were no strong retrospective patterns in the estimates of biomass and fishing mortality in base scenario. The negative Mohn's rho of biomass indicates that the estimate of biomass in a given year is more likely to be larger with more data added into the model. The adjusted estimate of the biomass or fishing mortality in terminal year could be calculated by *Base point**1/(1+*Mohn's rho*) (Deroba, 2014). The 2015 estimate of biomass and fishing mortality adjusted for retrospective pattern was showed in Figure 8.

Projection

A five-year projection was conducted from 2016 ~2020 for base scenario. 1, 1.5 and 2 times of the highest catch over the last three years and MSY were assumed to be the

annual catch for the projection. The simulations were done for 10000 times for each catch strategies. The probability of the stock being overfished was calculated (Table 6). Due to the uncertainty of dynamic process (sigma≠0), it is possible that the stock could be overfished even the annual catch is set below *MSY*. The probability of stock being overfished in next year (2016) is smaller than that of any further projection years in any given catch strategy. Setting a short-term quota for jumbo flying squid whose population dynamic process is susceptible to the environmental variation is better than setting a constant long-term quota.

Table 6. Probability of stock being overfished under different annual catch strategies during 2016~2020 for base scenario

Annual catch	2016	2017	2018	2019	2020
1* highest catch	0.0159	0.0347	0.0345	0.0366	0.0342
1.5* highest catch	0.017	0.0473	0.0465	0.0521	0.0513
2* highest catch	0.0269	0.0703	0.068	0.0745	0.0691
MSY	0.0515	0.117	0.1405	0.1565	0.1617

Summary

1. The jumbo flying squid stock in the Southeast Pacific is not overfished and overfishing does not occur. The current catch level is much lower than the estimated MSY and is sustainable.

2. The CPUE data from Chinese vessels may be a good proxy to represent the stock abundance outside the EEZ of Peru and Chile. The stock assessment model could be highly facilitated if the CPUE data or any other survey data within the EEZ of Peru and Chile are included.

3. The time series of 13 years may be short especially when retrospective pattern analysis need to be done by peeling years.

4. We simplified the complex population structure in this study. We plan to construct more sophisticated models to include size structure and/or possible meta-structure of the population and compare them with surplus production model. However, this can only be done if we have size composition and/or spatially-explicit catch and abundance index data which may become available if relevant parties work together.

5. As a short lived species, the population dynamics of jumbo flying squid can be significantly influenced by changes in their environment. Annual variability in environment may have equal or more influence on the dynamics of jumbo flying squid, compared with fishing pressure. Critical environmental factors should be taken into consideration to make a short-term management decision for jumbo flying squid in Southeast Pacific Ocean.

References

Arkhipkin, A., Argüelles, J., Shcherbich, Z., Yamashiro, C., 2014. Ambient temperature influences adult size and life span in jumbo squid (Dosidicus gigas). Can. J. Fish. Aquat. Sci. 72, 400–409.

Csirke, J., Alegre, A., Argüelles, J., Guevara-Carrasco, R., Mariátegui, L., Segura, M., Tafúr, R., Yamashiro, C., 2015. Main biological and fishery aspects of the jumbo squid (Dosidicus gigas) in the Peruvian Humboldt Current System, South Pacific Regional Fisheries Management Organization.

Deroba, J.J., 2014. Evaluating the Consequences of Adjusting Fish Stock Assessment Estimates of Biomass for Retrospective Patterns using Mohn's Rho. North Am. J. Fish. Manag. 34, 380–390.

Gelman, A., Rubin, D.B., 1992. Inference from Iterative Simulation Using Multiple Sequences. Comput. Stat. Data Anal. 7, 457–472.

Heidelberger, P., Welch, P.D., 1983. Simulation Run Length Control in the Presence of an Initial Transient Author. Oper. Res. 31, 1109–1144.

Hilborn, R., Walters, C.J., 1992. Quantitative Fisheries Stock Assessment, Marine Biology. Springer US, Boston, MA.

Liu, B., Chen, X., Chen, Y., Tian, S., Li, J., Fang, Z., Yang, M., 2013. Age, maturation, and population structure of the Humboldt squid Dosidicus gigas off the Peruvian Exclusive Economic Zones. Chinese J. Oceanol. Limnol. 31, 81–91.

McAllister, M.K., Kirkwood, G.P., 1998. Bayesian stock assessment: a review and example application using the logistic model. ICES J. Mar. Sci. 55, 1031–1060.

Mohn, R., 1999. The retrospective problem in sequential population analysis: An investigation using cod fishery and simulated data. ICES J. Mar. Sci. 56, 473–488.

Nigmatullin, C.M., Nesis, K.N., Arkhipkin, A.I., 2001. A review of the biology of the jumbo squid *Dosidicus gigas* (Cephalopoda: Ommastrephidae). Fish. Res. 54, 9–19.

Patterson, T.A., Thomas, L., Wilcox, C., Ovaskainen, O., Matthiopoulos, J., 2008. State-space models of individual animal movement. Trends Ecol. Evol. 23, 87–94.

Sandoval-Castellanos, E., Uribe-Alcocer, M., Díaz-Jaimes, P., 2010. Population genetic structure of the Humboldt squid (Dosidicus gigas d'Orbigny, 1835) inferred by mitochondrial DNA analysis. J. Exp. Mar. Bio. Ecol. 385, 73–78.

Yu, W., Yi, Q., Chen, X., Chen, Y., 2016. Modelling the effects of climate variability on habitat suitability of jumbo flying squid, Dosidicus gigas, in the Southeast Pacific Ocean off Peru. ICES J. Mar. Sci. 73, 239–249.

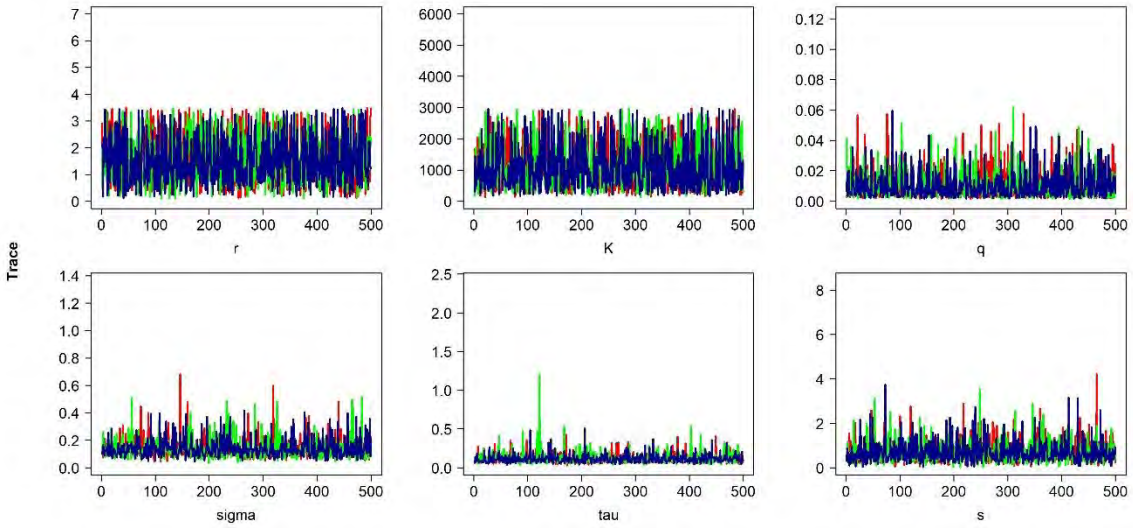

(a)

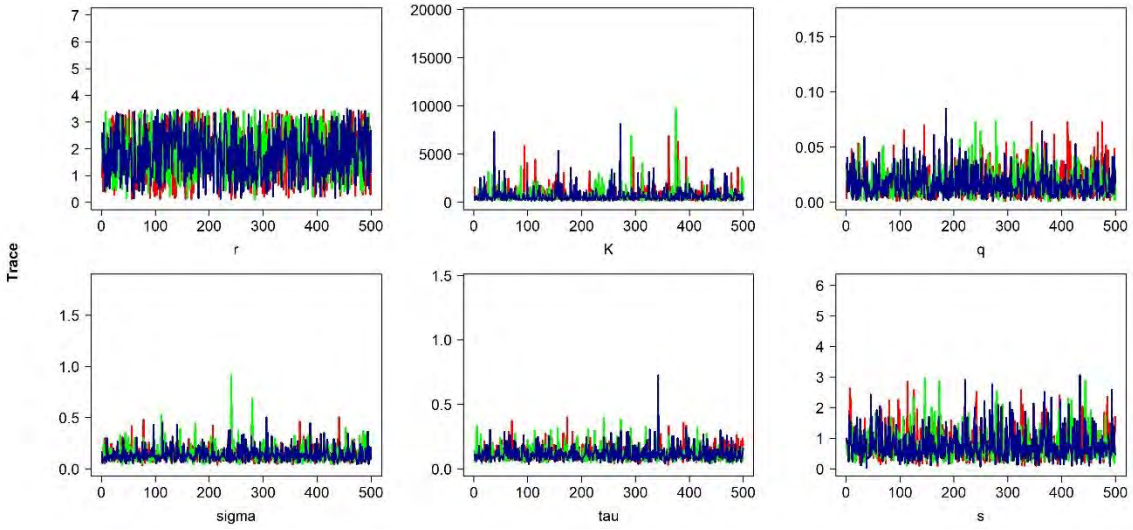

(b)

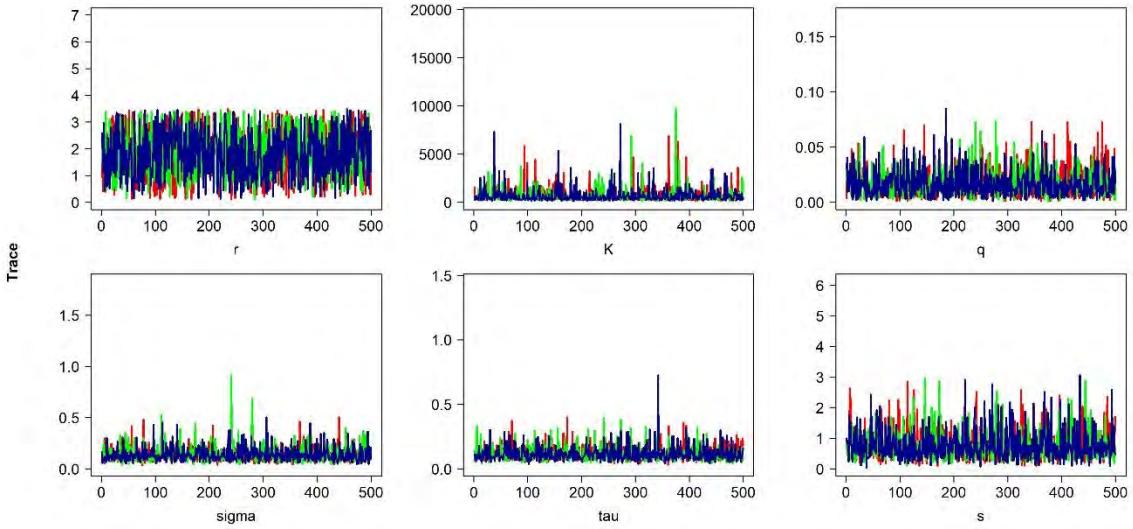

(c)

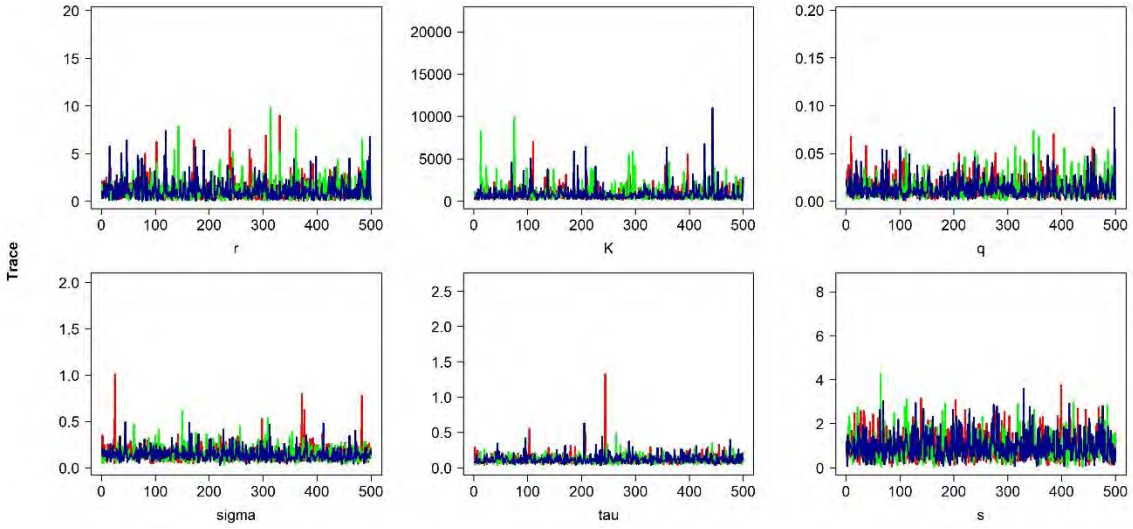

(d)

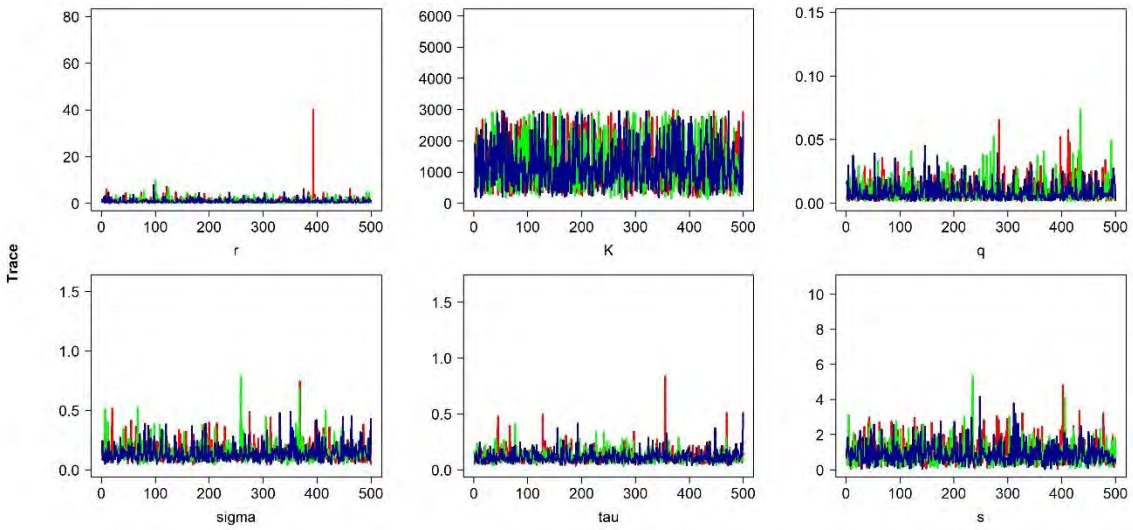

(e)

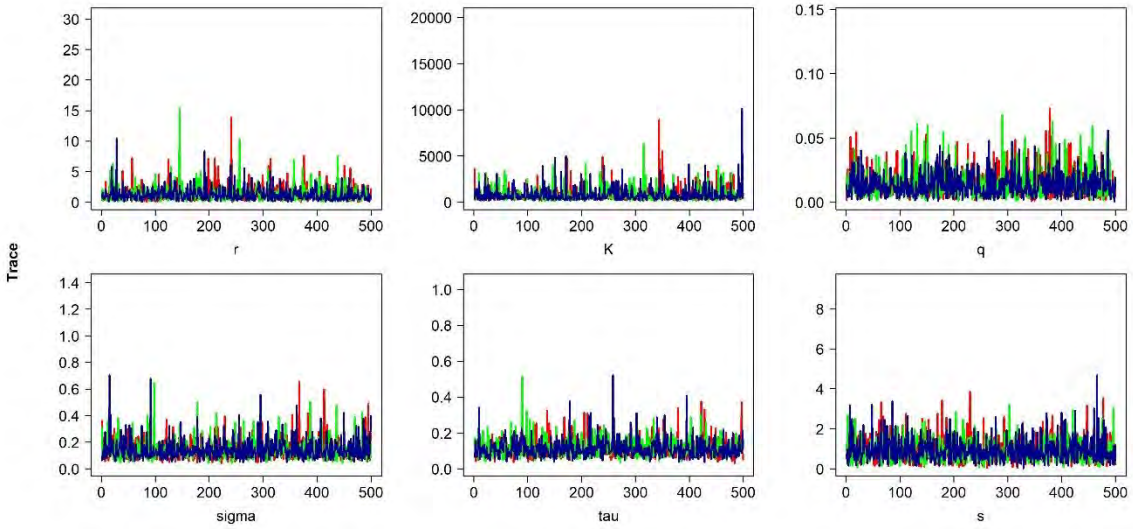

(f)

Figure 3. Trace of three chains of MCMC sample for posterior distributions of parameters in (a) base scenario; (b) sensitivity analysis scenario 1; (c) sensitivity analysis scenario 2; (d) sensitivity analysis scenario 3; (e) sensitivity analysis scenario 4; (f) sensitivity analysis scenario 5; the unit of k is 10^4 metric ton.

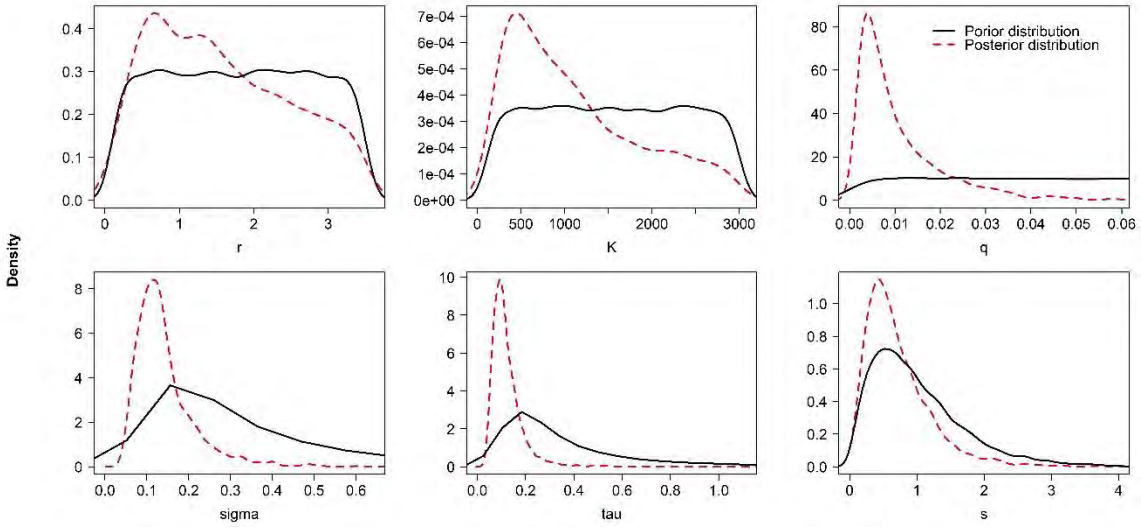
Density
r
K
q
sigma
tau
s
Porior distribution
Posterior distribution

(a)

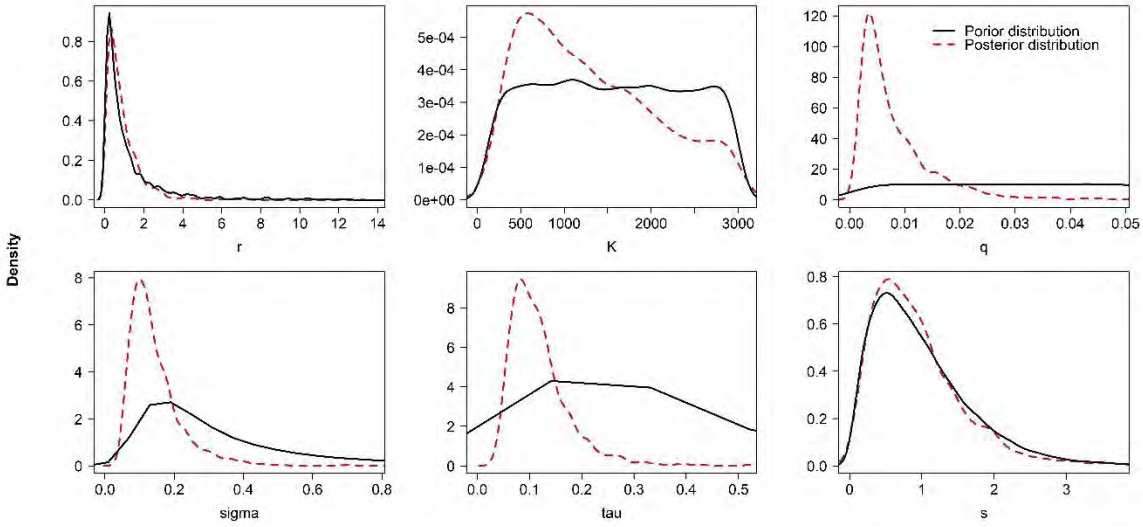
Density
r
K
q
sigma
tau
s
Porior distribution
Posterior distribution

(b)

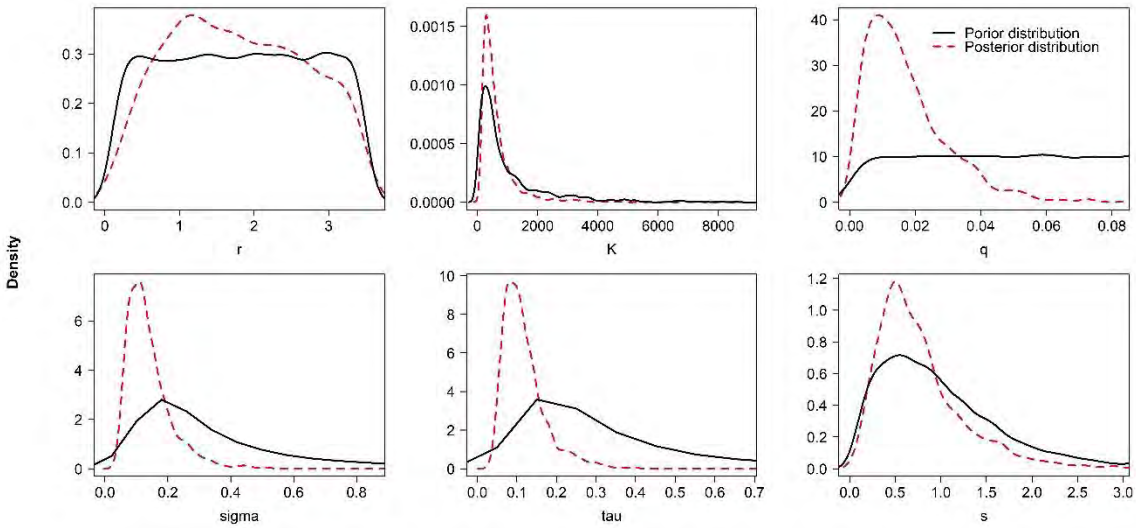
Density
r
K
q
sigma
tau
s
Porior distribution
Posterior distribution

(c)

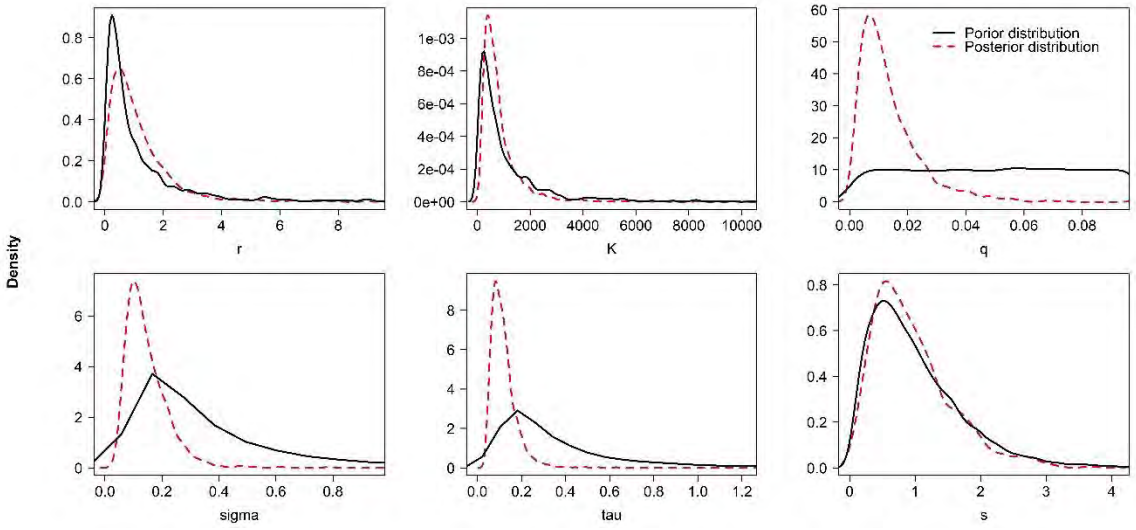
Density
r
K
q
sigma
tau
s
Porior distribution
Posterior distribution

(d)

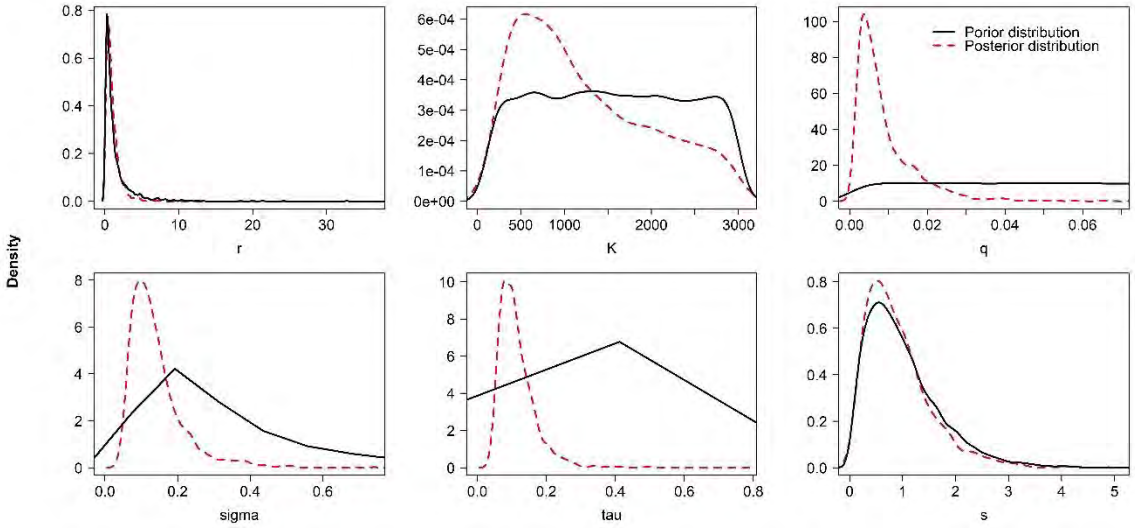

(e)

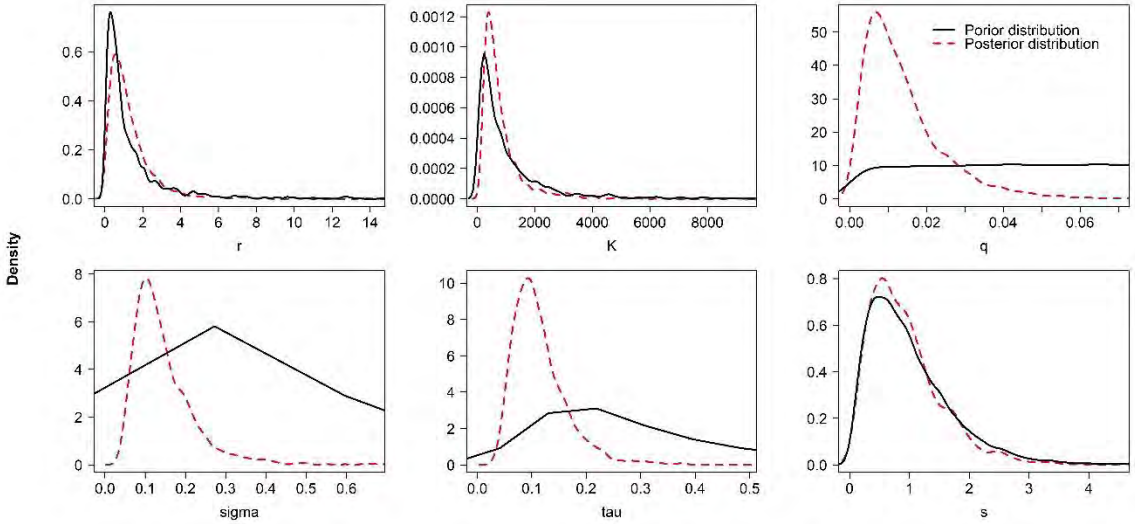

(f)

Figure 4. Prior and posterior distributions of parameters in (a) base scenario; (b) sensitivity analysis scenario 1; (c) sensitivity analysis scenario 2; (d) sensitivity analysis scenario 3; (e) sensitivity analysis scenario 4; (f) sensitivity analysis scenario 5; the unit of k is 10^4 metric ton.

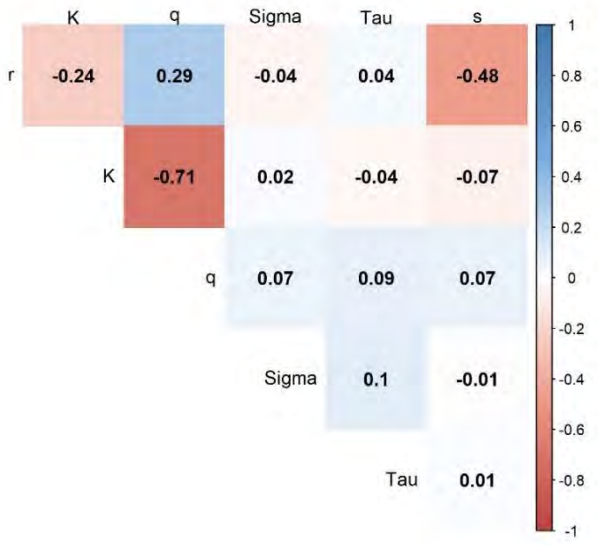
K
q
Sigma
Tau
s
r
-0.24
0.29
-0.04
0.04
-0.48
K
-0.71
0.02
-0.04
-0.07
q
0.07
0.09
0.07
Sigma
0.1
-0.01
Tau
0.01
1
0.8
0.6
0.4
0.2
0
-0.2
-0.4
-0.6
-0.8
-1

(a)


K
q
Sigma
Tau
s
r
-0.29
0.32
-0.04
-0.01
-0.31
K
-0.72
-0.01
0
-0.06
q
0.13
0
0.07
Sigma
0.14
-0.02
Tau
-0.04
1
0.8
0.6
0.4
0.2
0
-0.2
-0.4
-0.6
-0.8
-1

(b)

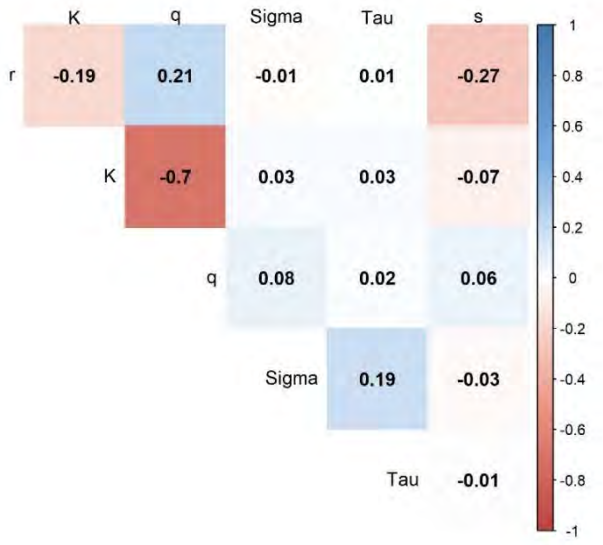
K
q
Sigma
Tau
s
r
-0.19
0.21
-0.01
0.01
-0.27
K
-0.7
0.03
0.03
-0.07
q
0.08
0.02
0.06
Sigma
0.19
-0.03
Tau
-0.01
1
0.8
0.6
0.4
0.2
0
-0.2
-0.4
-0.6
-0.8
-1

(c)

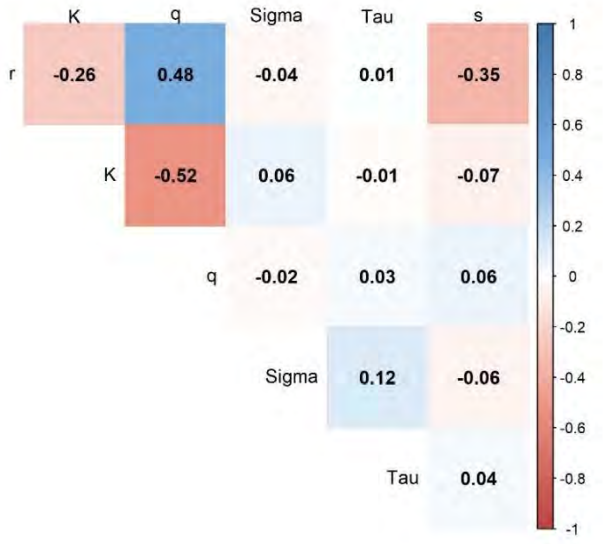
K
q
Sigma
Tau
s
r
-0.26
0.48
-0.04
0.01
-0.35
K
-0.52
0.06
-0.01
-0.07
q
-0.02
0.03
0.06
Sigma
0.12
-0.06
Tau
0.04
1
0.8
0.6
0.4
0.2
0
-0.2
-0.4
-0.6
-0.8
-1

(d)

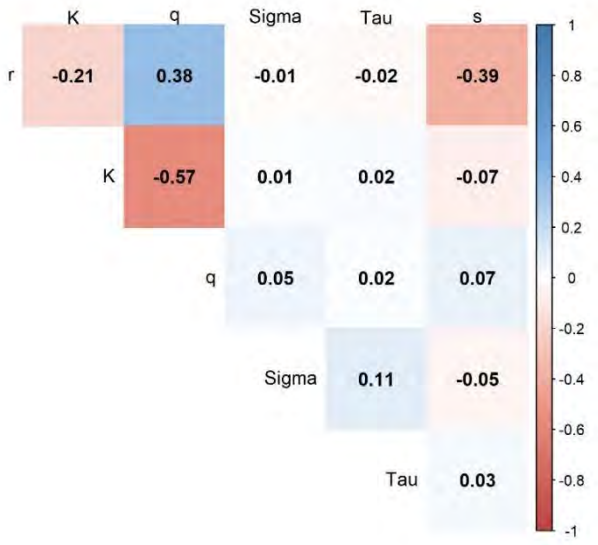

(e)

(f)

Figure 5. Correlation of parameters in (a) base scenario; (b) sensitivity analysis scenario 1; (c) sensitivity analysis scenario 2; (d) sensitivity analysis scenario 3; (e) sensitivity analysis scenario 4; (f) sensitivity analysis scenario 5

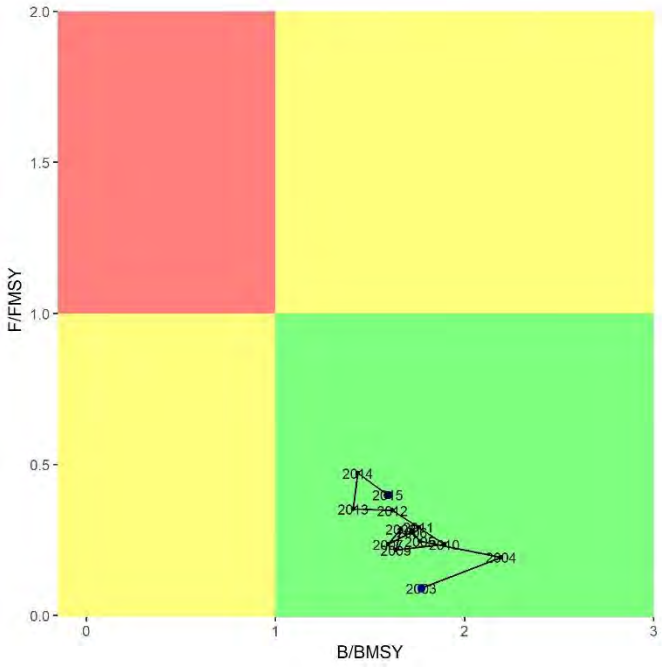
2.0
1.5
1.0
0.5
0.0
F/FMSY
0
1
2
3
B/BMSY
2014
2015
2013
2012
2004
2003

(a)

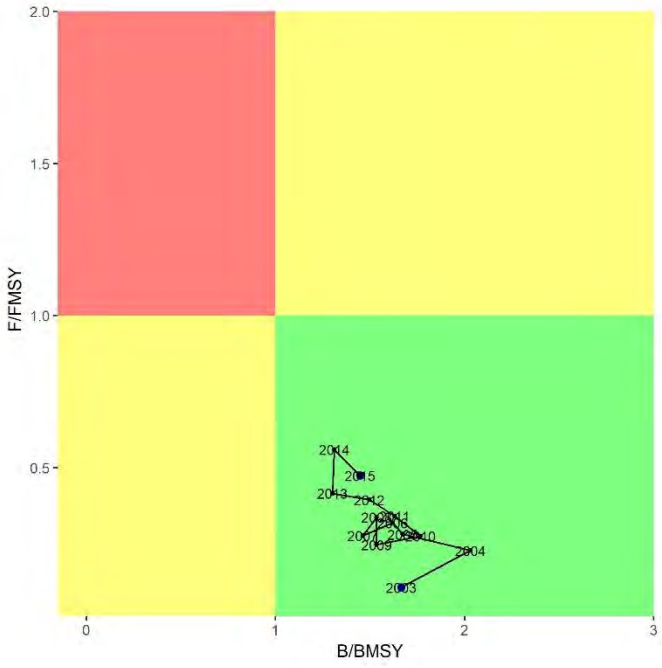
2.0
1.5
1.0
0.5
F/FMSY
0
1
2
3
B/BMSY
2014
2015
2013
2012
2004
2003

(b)

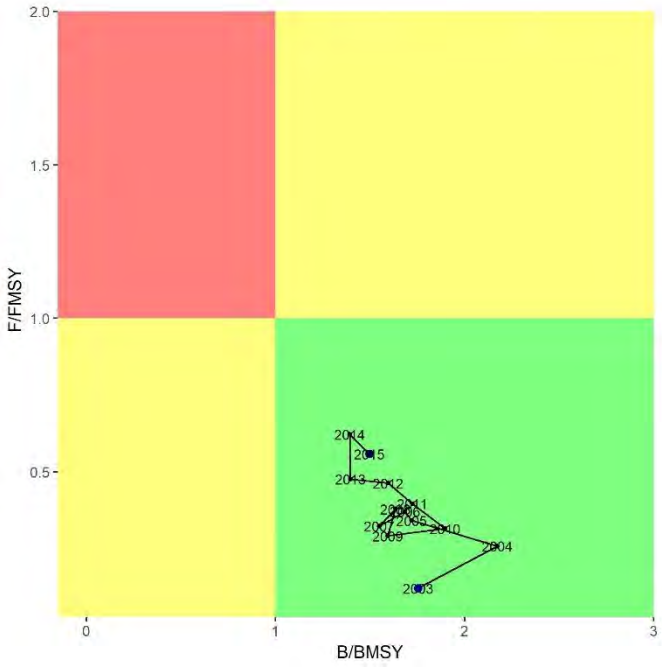
2.0
1.5
1.0
0.5
F/FMSY
2014
2015
2013
2012
2011
2010
2009
2004
2003
0
1
2
3
B/BMSY

(c)

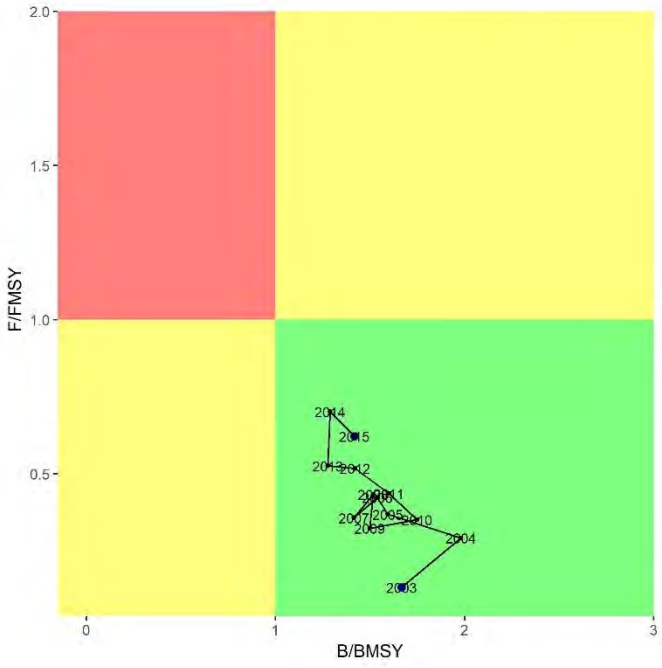
2.0
1.5
1.0
0.5
F/FMSY
2014
2015
2013
2012
2011
2010
2009
2004
2003
0
1
2
3
B/BMSY

(d)

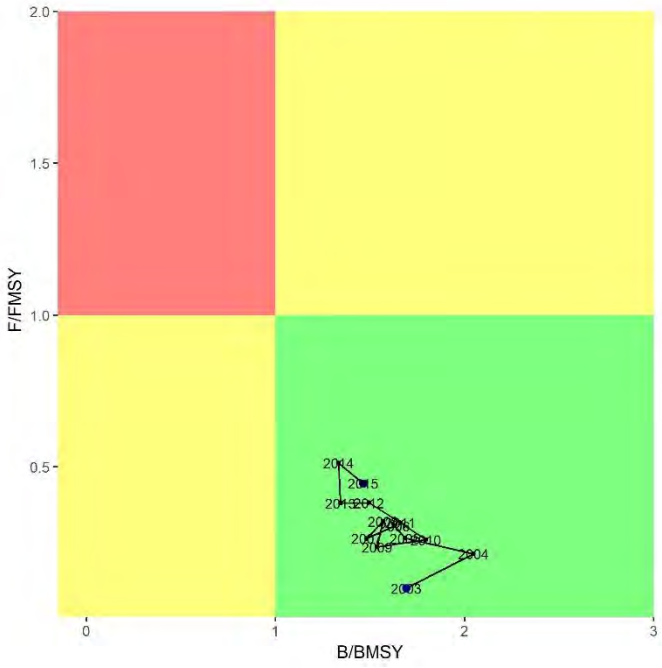

(e)

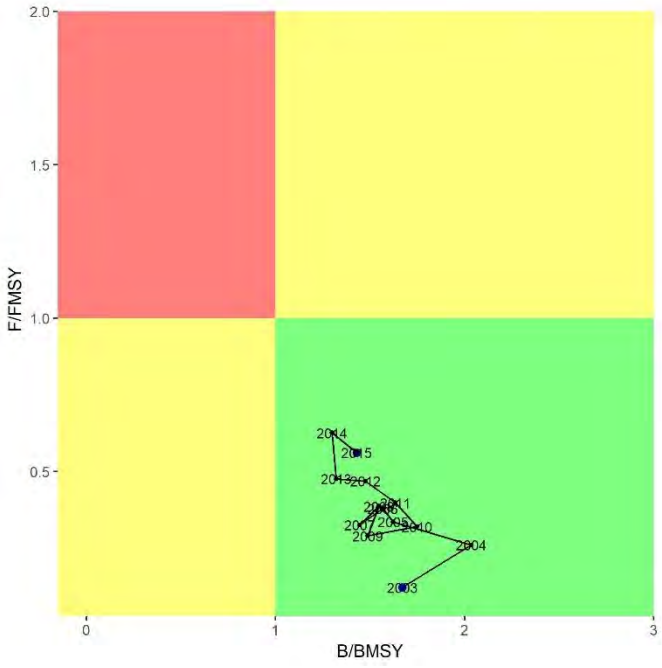

(f)

Figure 6. Kobe diagram of (a) base scenario; (b) sensitivity analysis scenario 1; (c) sensitivity analysis scenario 2; (d) sensitivity analysis scenario 3; (e) sensitivity analysis scenario 4; (f) sensitivity analysis scenario 5

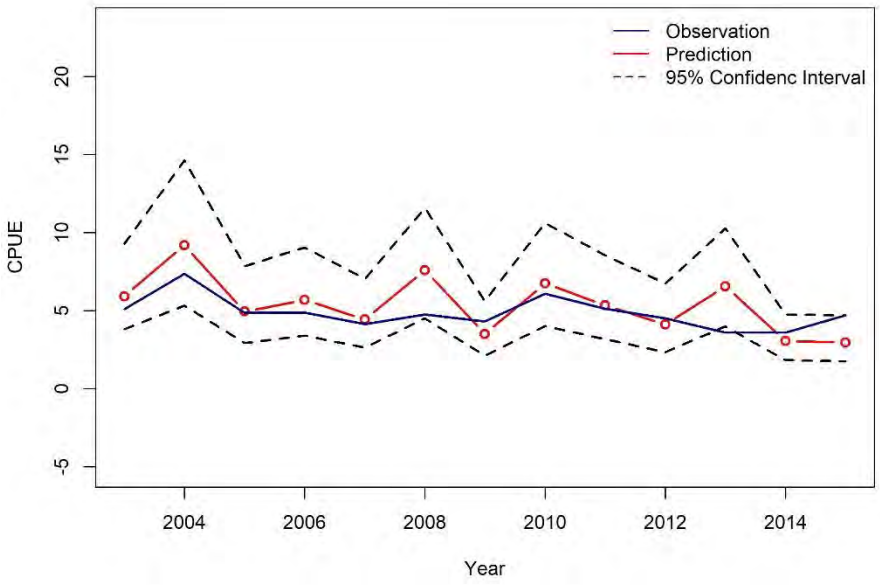
Observation
Prediction
95% Confidenc Interval
CPUE
-5
0
5
10
15
20
2004
2006
2008
2010
2012
2014
Year

(a)

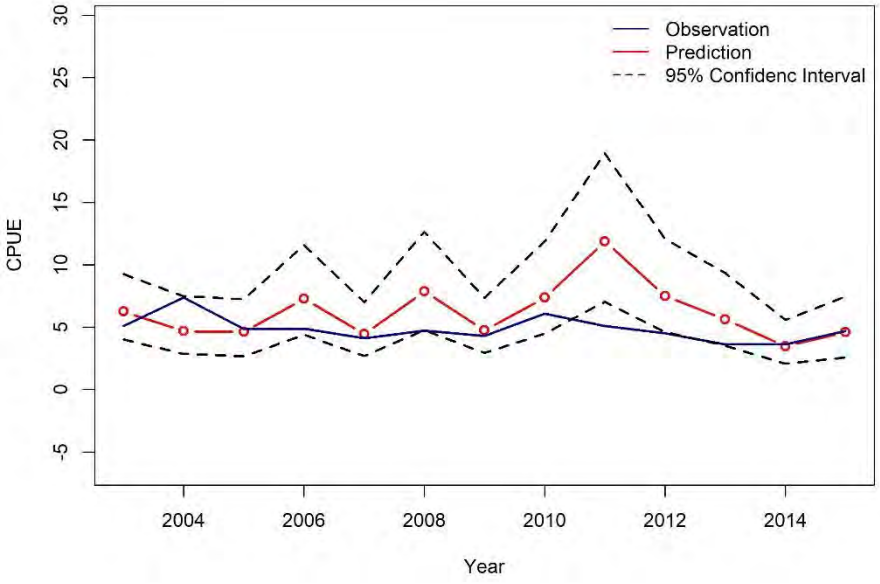
Observation
Prediction
95% Confidenc Interval
CPUE
-5
0
5
10
15
20
25
30
2004
2006
2008
2010
2012
2014
Year

(b)

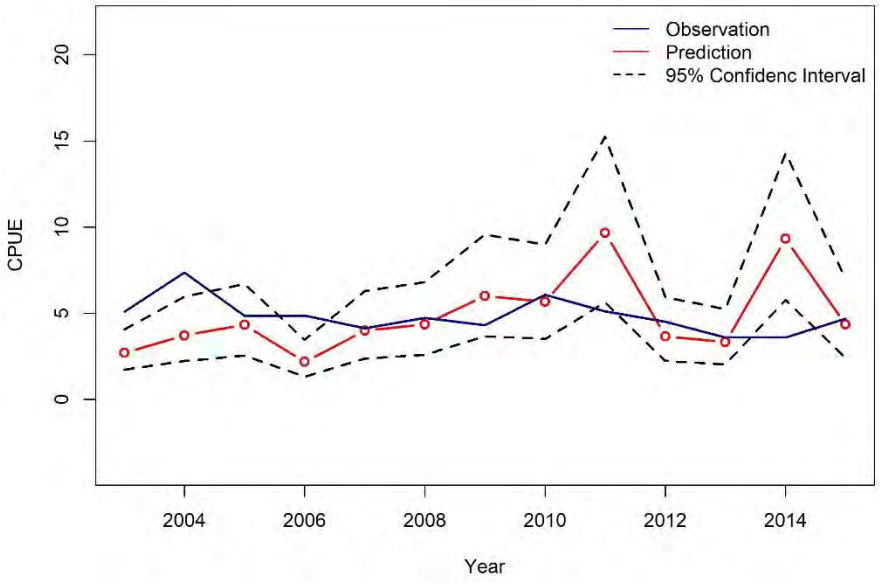
Observation
Prediction
95% Confidenc Interval
CPUE
0
5
10
15
20
2004
2006
2008
2010
2012
2014
Year

(c)

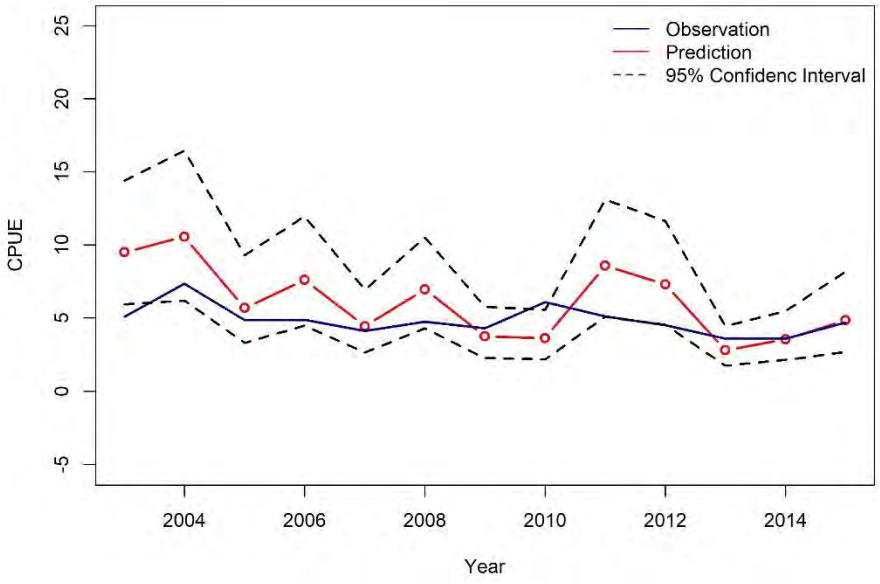
Observation
Prediction
95% Confidenc Interval
CPUE
-5
0
5
10
15
20
25
2004
2006
2008
2010
2012
2014
Year

(d)

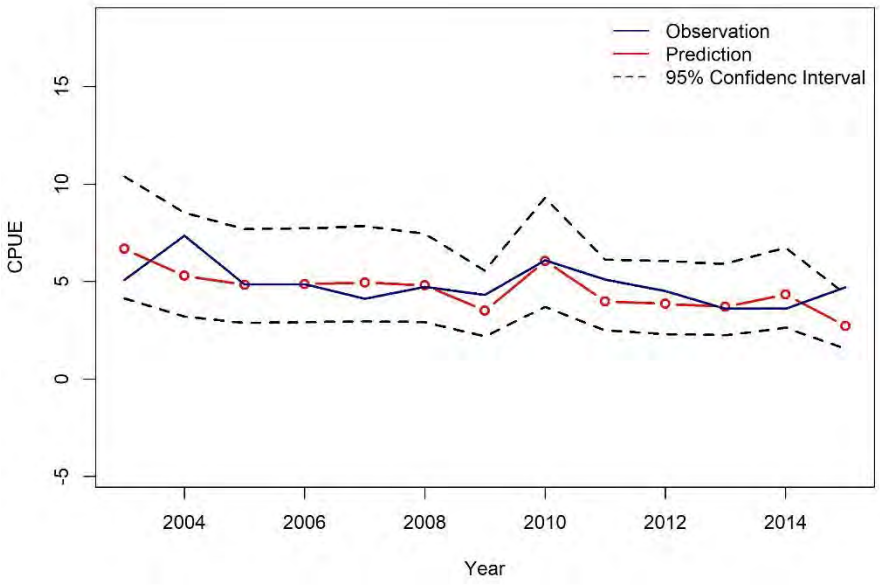

(e)

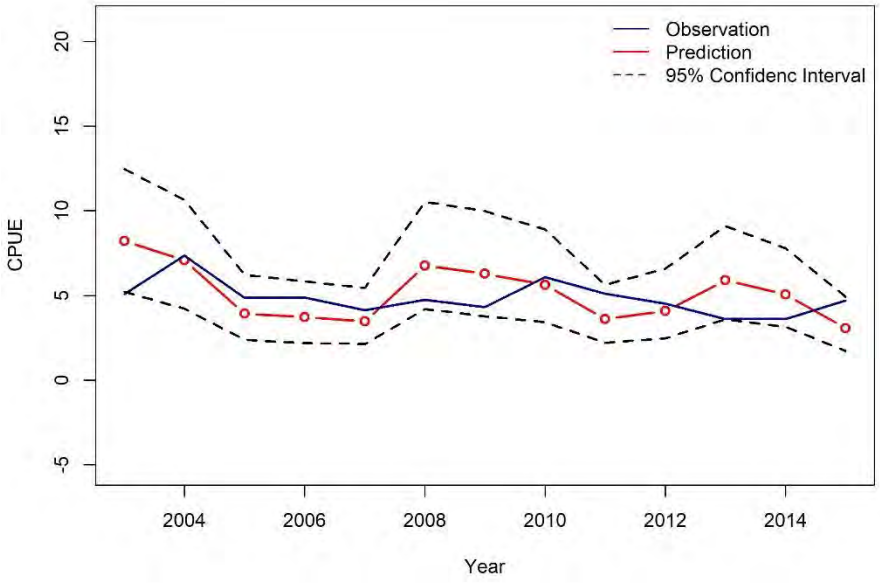

(f)

Figure 7. Temporal trend of observed and predicted CPUE index from (a) base scenario; (b) sensitivity analysis scenario 1; (c) sensitivity analysis scenario 2; (d) sensitivity analysis scenario 3; (e) sensitivity analysis scenario 4; (f) sensitivity analysis scenario 5; the unit of CPUE is metric ton/vessel/day.

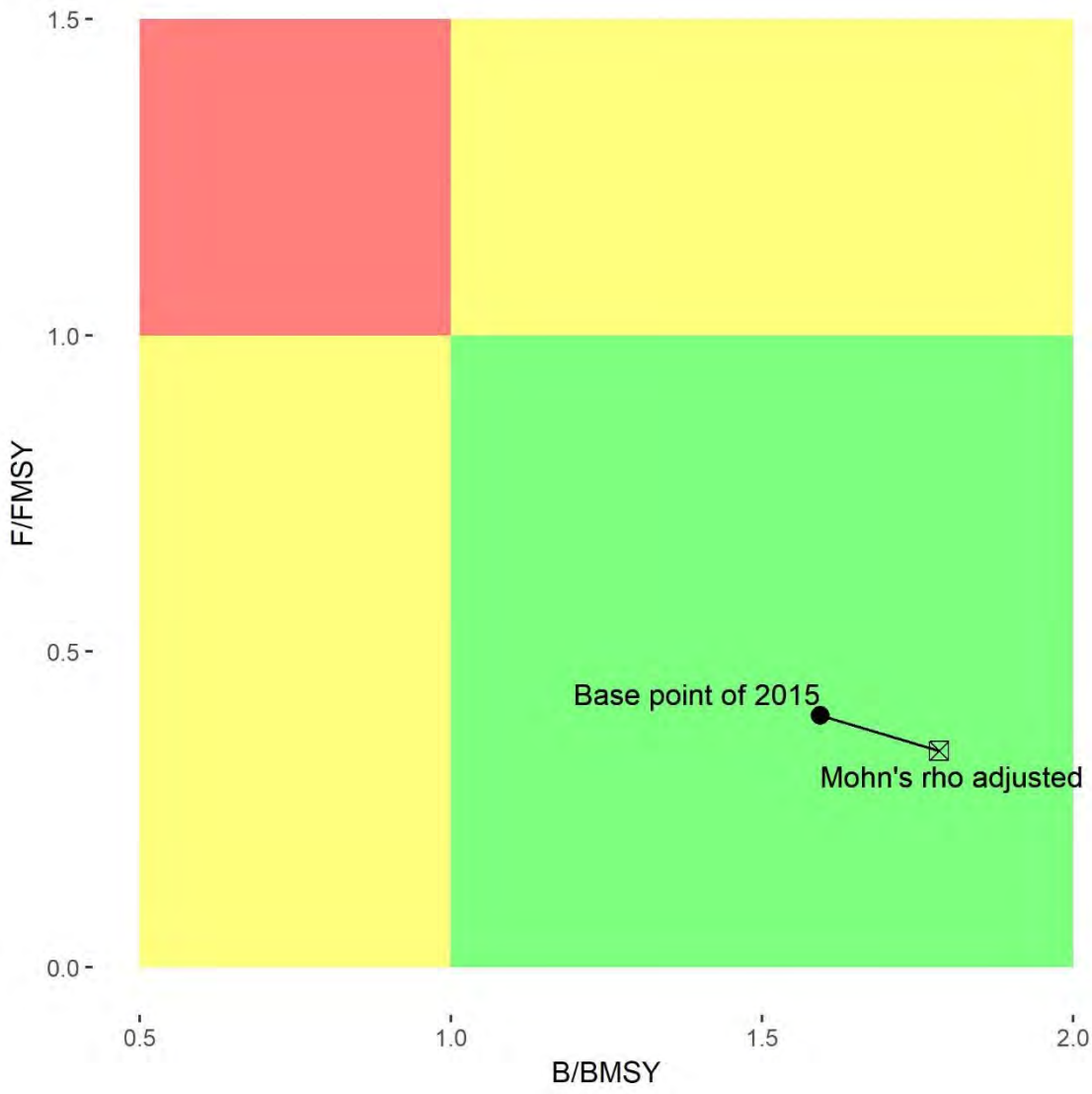

Figure 8. Base point of stock status of terminal year by base scenario of production model and the adjusted value based on Mohn's rho of fishing mortality and biomass.